

Divergence of Substrate Specificity and Function in the *Escherichia coli* Hotdog-fold Thioesterase Paralogs YdiI and YdbB

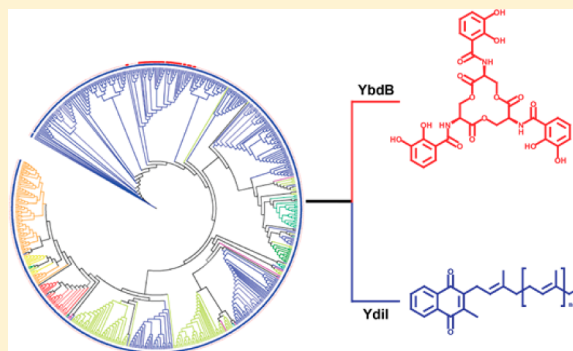
John A. Latham,[†] Danqi Chen,[†] Karen N. Allen,[‡] and Debra Dunaway-Mariano^{*,†}

[†]Department of Chemistry & Chemical Biology, University of New Mexico, Albuquerque, New Mexico 87131, United States

[‡]Department of Chemistry, Boston University, Boston, Massachusetts 02215, United States

S Supporting Information

ABSTRACT: The work described in this paper, and its companion paper (Wu, R., Latham, J. A., Chen, D., Farelli, J., Zhao, H., Matthews, K. Allen, K. N., and Dunaway-Mariano, D. (2014) Structure and Catalysis in the *Escherichia coli* Hotdog-fold Thioesterase Paralogs YdiI and YdbB. *Biochemistry*, DOI: 10.1021/bi500334v), focuses on the evolution of a pair of paralogous hotdog-fold superfamily thioesterases of *E. coli*, YdbB and YdiI, which share a high level of sequence identity but perform different biological functions (viz., proofreader of 2,3-dihydroxybenzoyl-*holoEntB* in the enterobactin biosynthetic pathway and catalyst of the 1,4-dihydroxynaphthoyl-CoA hydrolysis step in the menaquinone biosynthetic pathway, respectively). In vitro substrate activity screening of a library of thioester metabolites showed that YdbB displays high activity with benzoyl-*holoEntB* and benzoyl-CoA substrates, marginal activity with acyl-CoA thioesters, and no activity with 1,4-dihydroxynaphthoyl-CoA. YdiI, on the other hand, showed a high level of activity with its physiological substrate, significant activity toward a wide range of acyl-CoA thioesters, and minimal activity toward benzoyl-*holoEntB*. These results were interpreted as evidence for substrate promiscuity that facilitates YdbB and YdiI evolvability, and divergence in substrate preference, which correlates with their assumed biological function. YdiI support of the menaquinone biosynthetic pathway was confirmed by demonstrating reduced anaerobic growth of the *E. coli ydiI*-knockout mutant (vs wild-type *E. coli*) on glucose in the presence of the electron acceptor fumarate. Bioinformatic analysis revealed that a small biological range exists for YdbB orthologs (i.e., limited to Enterobacteriales) relative to that of YdiI orthologs. The divergence in YdbB and YdiI substrate specificity detailed in this paper set the stage for their structural analyses reported in the companion paper.



The physiological roles of cellular thioesterases are centered on the catalyzed hydrolysis of thioester metabolites to their corresponding organic acid and thiol components. Thioesters are prevalent in the cell wherein they serve as activated forms of organic acids in a wide range of anabolic and catabolic chemical pathways. Thioesterases act on the thioester precursors,³ intermediates,⁴ or products⁵ of such pathways; alternatively, they perform supportive roles as proofreaders,⁶ housekeepers,^{7,8} or regulators.^{9,10}

Thioesterases belong primarily to the hotdog-fold or α,β -hydrolase-fold protein superfamilies.^{11,12} The hotdog-fold thioesterases possess a characteristic core structure consisting of a 5-turn α -helix cradled by a curved, 5-stranded antiparallel β -sheet.¹³ Dimerization forms an elongated β -sheet and two active sites located at opposite ends of the subunit interface. The topology of the substrate-binding site restricts catalytic activity to thioesters in which the thiol unit is coenzyme A (CoA) or a phosphopantetheine-functionalized acyl carrier protein (*holoACP*).¹⁴ In contrast, the substrate range covered by the thioesterase family of the α,β -hydrolase-fold protein superfamily also includes cysteine-linked thioesters (e.g., palmitoylated proteins).¹⁵

The largest family within the hotdog-fold protein superfamily is comprised of thioesterases, principally because of the large demand for thioester hydrolysis in the cell. The prevalence of the hotdog-fold thioesterase family, in particular, suggests high evolvability, meaning that the hotdog-fold scaffold readily takes on new functions. It is well-known that substrate promiscuity is a key factor in the rapid gain of novel biological function (for a recent review of this topic, see ref 16). The intrinsic promiscuity of a hotdog-fold thioesterase can be revealed through determination of its substrate specificity profile by in vitro substrate activity screening. Herein, we examine the substrate specificities of a pair of hotdog-fold thioesterase family paralogs,^a *Escherichia coli* YdbB and YdiI, to discover that although they are intrinsically promiscuous, they display high catalytic efficiency for, and discrimination between, their respective physiological substrates (viz., aberrant aroyl-*holoEntB*^b thioesters sometimes formed as dead-end adducts during enterobactin biosynthesis^{1,6,17} and 1,4-dihydroxynap-

Received: March 18, 2014

Revised: June 26, 2014

Published: July 3, 2014

thoyl-CoA formed as an intermediate of the menaquinone biosynthetic pathway^{4,18–20}). In addition, we used bioinformatic methods to identify and map the biological ranges of YbdB and YdiI orthologs and site-directed mutagenesis to evaluate potential sequence markers. In the companion paper,² we report on the structure and mechanism *E. coli* YbdB and YdiI.

MATERIALS AND METHODS

The restriction enzymes, T4 DNA ligase, oligonucleotide primers, and the competent *E. coli* BL21(DE3) cells were purchased from Invitrogen. *Pfu Turbo* and *Deep Vent* DNA polymerases were purchased from Stratagene. The cloning vectors were from Novagen. DNA sequencing was performed by the DNA Sequencing Facility of the University of New Mexico. Acetyl-CoA, benzoyl-CoA, propanoyl-CoA, hexanoyl-CoA, lauroyl-CoA, myristoyl-CoA, palmitoyl-CoA, and oleoyl-CoA were purchased from Sigma. The thioester substrates 4-hydroxybenzoyl-CoA, 3-hydroxybenzoyl-CoA, 1,4-dihydroxynaphthoyl-CoA, 3-hydroxyphenylacetyl-CoA, and coumaroyl-CoA were synthesized as previously reported.^{18,21} *E. coli* strains JW1676 ($\Delta ydiI::kan^r$) and BW25113 (wild-type) of the Keio collection were obtained from Yale University.²² The engineered *E. coli* strain DKS74, carrying the plasmid pJT93 expressing the *E. coli* AcpS transferase gene, under *tac*-promoter control, was a kind gift from Dr. John Cronan of the University of Illinois. The *holoACP* (UniProt accession code P0A6A8) purified from this strain was converted to benzoyl-holoACP by using the chemical procedure reported in ref 23. The molecular mass and purity of the isolated adduct were verified by ES-MS analysis.

Growth Curve Measurements for Wild-Type and *ydiI*-Knockout *E. coli* Strains. Aerobic growth curves were carried out in sterile vented flasks (Nalgene) each containing 50 mL of M9 minimal media supplemented with 4% glucose as the sole carbon source, and with or without added kanamycin. An aliquot of a liquid culture of JW1676 (*ydiI*-knockout strain) or BW25113 (wild-type strain) *E. coli* cells grown overnight in LB broth was added to the media to an initial $A_{600} \sim 0.01$. Cultures were incubated at 37 °C with orbital shaking at 180 rpm. The culture A_{600} was determined at 1 h intervals for 14 h. Anaerobic growth curves were measured in a similar fashion using 50 mL of M9 minimal media supplemented with double the amount of phosphate and with 4% glucose plus 4% fumarate. The sterile flasks were capped with sterilized stoppers and purged for 2 min with N_2 gas passed through a sterile 0.2 μm in-line filter. Aliquots were removed by syringe, hourly over a 12 h period, for A_{600} determination.

Cloning, Expression, and Purification of C-terminus His-Tagged YbdB and YdiI. The genes encoding YbdB (UniProt accession code P0A8Y8) and YdiI (UniProt accession code P77781) were cloned by using a PCR-based strategy in which genomic DNA prepared from *E. coli* strain K12 (substrain W3110) was used as template, commercial oligonucleotides as the primers, and *Pfu Turbo* as the DNA polymerase. The *NdeI* and *XhoI*-treated PCR product was ligated, using T4 DNA ligase, to *NdeI/XhoI* sites of pET-23a (Novabiochem) to give the plasmids, *ybdB-His₆/pET-23a* and *ydiI-His₆/pET-23a*. The resulting clones were used to transform competent *E. coli* BL21 (DE3) cells (Novagen). The cells were grown at 37 °C in LB medium containing 50 $\mu g/mL$ of ampicillin. The cell culture was induced with 0.4 mM isopropyl- β -D-galactopyranoside (IPTG) once the optical density had

reached 0.6 (OD at 600 nm). Following an overnight induction at 20 °C, the cells were harvested by centrifugation at 5000g for 15 min. The cell pellet was suspended in 150 mL of lysis buffer (20 mM Tris-HCl, 10 mM imidazole, 1 mM DTT, and 300 mM NaCl, pH 7.5) and passed through a French pressure cell at 1200 psi before centrifugation at 48 000g for 1 h at 4 °C. The supernatant was loaded onto a Ni-NTA column (2 cm \times 11 cm), pre-equilibrated with lysis buffer. The column was washed at a flow rate of 0.5 mL/min with 150 mL of lysis buffer followed by 100 mL of wash buffer (20 mM Tris-HCl, 300 mM NaCl, 50 mM imidazole at pH 7.5). The His₆-tagged proteins were eluted with 90 mL of elution buffer (20 mM Tris-HCl, 300 mM NaCl, 250 mM imidazole at pH 7.5). The protein fractions were analyzed by SDS-PAGE before pooling, concentrating, and dialyzing (50 mM Tris-HCl, 100 mM NaCl at pH 7.5). Aliquots of the protein solutions were frozen for storage at –80 °C. Yield: ~ 15 mg of His₆-YbdB/g wet cell paste and ~ 10 mg of His₆-YdiI/g wet cell paste.

Preparation of YbdB and YdiI Site-Directed Mutants.

Site-directed mutagenesis was carried out using the Quik-Change PCR strategy (Stratagene) and the *ydiI-His₆/pET-23a* or *ybdB-His₆/pET-23a* plasmid as template with commercial primers and *Pfu Turbo* as the polymerase. The sequence of the mutated gene was confirmed by DNA sequencing. The recombinant mutant plasmids were used to transform competent *E. coli* BL21 Star (DE3) cells. The His₆-tagged mutant proteins YbdB M68V and YdiI V68M and F50A were purified to >90% homogeneity (as determined by SDS-PAGE analysis) as described above in a yield of ~ 10 –25 mg protein/g wet cell paste.

Determination of Steady-State Kinetic Constants.

Thioesterase activity was measured using a 5,5'-dithio-bis(2-nitrobenzoic acid) (DTNB) coupled assay. Reactions were monitored at 412 nm ($\Delta\epsilon = 13.6$ mM^{–1}·cm^{–1}) using a Beckman 640U spectrometer. Reactions were carried out 25 °C with 0.5 mL solutions containing 50 mM K⁺HEPES (pH 7.5), 1 mM DNTB, an optimal concentration of thioesterase, and varying concentrations of the substrate (0.5K_m to 5K_m). The catalyzed hydrolysis of 4-HB-CoA in 50 mM K⁺HEPES (pH 7.5) was directly monitored at 300 nm ($\Delta\epsilon = 11.8$ mM^{–1}·cm^{–1}). The initial velocity data, measured as a function of substrate concentration, were analyzed using Enzyme Kinetics v 1.4 and eq 1:

$$v = V_{\max}[S]/([S] + K_m) \quad (1)$$

where v is initial velocity, V_{\max} is maximum velocity, $[S]$ is substrate concentration, and K_m is the Michaelis constant. The k_{cat} was calculated from $V_{\max}/[E]$ where $[E]$ is the total enzyme concentration as determined by the Bradford method.²⁴

Determination of YbdB and YdiI pH-Rate Profiles for Catalyzed 4-HB-CoA Thioester Hydrolysis.

The initial velocities of YbdB and YdiI-catalyzed hydrolysis of 4-HB-CoA, at varying concentration (in the range of 0.5K_m to 5K_m), were measured at 25 °C (vide supra). The pH values of the reaction solutions were maintained using 50 mM MES, HEPES, TAPS, or CAPSO. Control reactions, in which the enzyme was preincubated in the reaction buffer and then assayed at pH 7.5, were carried out to detect possible inactivation at the pH extremes.

Bioinformatic Analysis. BLAST searches of the sequenced genomes deposited in NCBI were carried out using the Genomics Groups BLAST server (http://www.ncbi.nlm.nih.gov/sutils/genom_table.cgi). The *E. coli* K12 YbdB and YdiI

Table 1. Steady-State Kinetic Parameters of YbdB- and YdiI-Catalyzed Hydrolysis of Various Acyl-CoA, Aryl-CoA, Aryl-Holo-ACP, or Aryl-holo-EntB Substrates at pH 7.5 and 25 °C^a

substrate ^b	YdiI			YbdB ^b		
	k_{cat} (s ⁻¹)	K_{m} (μM)	$k_{\text{cat}}/K_{\text{m}}$ (M ⁻¹ s ⁻¹)	k_{cat} (s ⁻¹)	K_{m} (μM)	$k_{\text{cat}}/K_{\text{m}}$ (M ⁻¹ s ⁻¹)
acetyl-CoA	$<1 \times 10^{-4}$	ND ^d	ND ^d	$(4.4 \pm 0.2) \times 10^{-3b}$	800 ± 90	5.5
propionyl-CoA	$(2.1 \pm 0.1) \times 10^{-1}$	120 ± 10	1.7×10^3	$(1.3 \pm 0.1) \times 10^{-2b}$	400 ± 40	3.1×10^1
β-methylcrotonyl-CoA	$(5.0 \pm 0.2) \times 10^{-1}$	69.4 ± 0.4	7.3×10^3	ND ^d	ND ^d	ND ^d
β-methylmalonyl-CoA	$(6.7 \pm 0.3) \times 10^{-1}$	115 ± 7	5.8×10^3	ND ^d	ND ^d	ND ^d
hexanoyl-CoA	$(3.0 \pm 0.1) \times 10^{-1}$	21 ± 1	1.4×10^4	$(1.4 \pm 0.1) \times 10^{-1b}$	260 ± 20	5.2×10^2
decanoyl-CoA	ND ^d	ND ^d	ND ^d	$(2.7 \pm 0.1) \times 10^{-2b}$	45 ± 2	5.4×10^2
lauroyl-CoA	$(7.4 \pm 0.1) \times 10^{-1}$	2.2 ± 0.1	3.3×10^5	$(2.8 \pm 0.1) \times 10^{-2b}$	44 ± 2	6.2×10^2
myristoyl-CoA	$(6.2 \pm 0.1) \times 10^{-1}$	1.5 ± 0.2	4.1×10^5	$(7.8 \pm 0.3) \times 10^{-2}$	11 ± 1	7.1×10^3
palmitoyl-CoA	$(5.8 \pm 0.1) \times 10^{-1}$	1.9 ± 0.1	3.0×10^5	$(8.5 \pm 0.3) \times 10^{-2b}$	55 ± 9	1.5×10^3
oleoyl-CoA	$(1.2 \pm 0.1) \times 10^{-1}$	1.3 ± 0.1	9.2×10^4	$(3.0 \pm 0.2) \times 10^{-2}$	13 ± 2	2.3×10^3
benzoyl-CoA	17.7 ± 0.7	25 ± 3	7.1×10^5	2.2 ± 0.2	12 ± 1	1.8×10^5
4-HB-CoA	5.2 ± 0.2	9 ± 1	5.8×10^5	1.6 ± 0.1 ^b	21 ± 2	7.6×10^4
3-HB-CoA	ND ^d	ND ^d	ND ^d	1.2 ± 0.01 ^b	37 ± 1	3.4×10^4
1,4-DHN-CoA	1.6 ± 0.1	8 ± 1	2.0×10^5	$(9.3 \pm 0.2) \times 10^{-3}$	17 ± 1	5.5×10^2
3-HPA-CoA	ND ^d	ND ^d	ND ^d	2.1 ± 0.5 ^b	37 ± 1	5.7×10^4
coumaroyl-CoA	8.4 ± 0.2	30 ± 2	2.8×10^5	$(8.2 \pm 0.2) \times 10^{-1}$	10 ± 1	8.2×10^4
2,4-DHB-EntB	3.6×10^{-3}	200 ± 20	1.8×10^1	3.7 ± 0.1 ^b	25 ± 1	1.4×10^5
2,3-DHB-EntB	ND ^d	ND ^d	ND ^d	2.8 ± 0.1 ^b	15 ± 1	1.8×10^5
lauroyl-EntB	ND ^d	ND ^d	ND ^d	$(1.0 \pm 0.01) \times 10^{-1b}$	32 ± 2	6.3×10^2
benzoyl-ACP	$(8.3 \pm 0.7) \times 10^{-2}$	54 ± 5	1.5×10^3	$(1.3 \pm 0.1) \times 10^{-2}$	60 ± 10	2.2×10^2

^aSee Materials and Methods for details. ^bKinetic constants are from ref 17. ^cAbbreviations: HB-CoA, hydroxybenzoyl-CoA; DHN-CoA, dihydroxynaphthoyl-CoA; HPA-CoA, hydroxyphenylacetyl-CoA; DHB-EntB, dihydroxybenzoyl-EntB. ^dND stands for not determined.

sequences were used as queries, as were the sequences of the *E. coli* enterobactin and menaquinone biosynthetic pathway enzymes. Protein sequence alignments were generated using COBALT (www.ncbi.nlm.nih.gov/tools/cobalt/)²⁵ and displayed in ESPrit3 (<http://espriti.ibcp.fr/ESPrIt/ESPrIt/index.php>).²⁶ Pathway gene context was determined by browsing gene neighborhoods in PATRIC (<http://patric.vbi.vt.edu/>) and EnsemblBacteria (<http://bacteria.ensembl.org/index.html>). Homologs of the *E. coli* YbdB and YdiI were identified for each bacterial phylum by carrying out BLAST searches of deposited genomes, one genus at a time. *E. coli* YdiI and YbdB homologs having >35% sequence identity for >80% sequence coverage when aligned pairwise with the YdiI sequence are listed in Table S11 of the Supporting Information. The genomes of the order Enterobacteriales were examined one species at a time using *E. coli* YbdB or YdiI as query in parallel BLAST searches. We found one, two, or zero closely related sequence homologs (viz., >50% sequence identity for >85% coverage) for each of the 92 genomes. To distinguish between YbdB or YdiI orthologs, we compared pairwise sequence identities (viz., homolog vs *E. coli* YbdB and homolog vs *E. coli* YdiI; higher sequence identity associated with the orthologous pair) and we checked for evidence of encoded enterobactin and menaquinone pathway enzymes by carrying out BLAST searches using the sequences of the respective pathway enzymes as queries.

RESULTS AND DISCUSSION

pH Dependence of YbdB and YdiI Catalytic Efficiency.

The variation in k_{cat} and $k_{\text{cat}}/K_{\text{m}}$ values for YdiI and YbdB-catalyzed thioester hydrolysis as a function of reaction solution pH was measured for the purpose of defining the optimal pH range for catalysis. 4-Hydroxybenzoyl-CoA (4-HB-CoA) was selected to serve as the substrate in the pH rate profile determinations because it is a highly active substrate for both

enzymes (see Table 1), and its reaction can be monitored directly and continuously by measuring the decrease in solution absorbance (at 300 nm) associated with the cleavage of its *para*-hydroxyphenyl-conjugated thioester group.²⁷ As illustrated in Figure 1, the k_{cat} and $k_{\text{cat}}/K_{\text{m}}$ values measured for YbdB are maximal at or near neutral pH, whereas both drop at acidic and at basic pH. This trend was also noted by Guo and co-workers for YbdB-catalyzed 2-hydroxybenzoyl-CoA and 2,3-dihydroxybenzoyl-CoA hydrolysis.¹ The YdiI $k_{\text{cat}}/K_{\text{m}}$ value decreases below pH 6.5 and above 8.5, whereas the k_{cat} value is relatively constant above pH 6.5 but then decreases with decreasing pH.

The pH-dependences of YdiI and YbdB catalysis are similar but not identical. The kinetic experiments reported below were carried out at a solution pH of 7.5 because both enzymes are fully active and stable at this pH, and the DTNB-based assay for continuous monitoring via coupled reaction with the CoA thiolate anion could be used in the determination of the substrate specificity profiles (see below).

YbdB and YdiI Substrate Specificity Profiles. The steady-state rate constants k_{cat} and K_{m} were determined for YbdB- and YdiI-catalyzed hydrolysis of a structurally diverse library of thioesters for the purpose of evaluating selectivity toward the thiol moiety (CoA vs *holo*ACP)² and toward the acyl or aroyl moiety (see Chart 1 for chemical structures). The CoA thioesters represent various classes of metabolites, differing in the size, shape, and polarity of the acyl/aroyl group. The acyl carrier protein (ACP)-based thioesters were used to test recognition of the *holo*ACP of the *E. coli* fatty acid synthetic (FAS) pathway²⁸ and the *holo*ACP domain of EntB of the *E. coli* enterobactin synthetic pathway²⁹ (Figure 2A).

The physiological substrate for YbdB (aka EntH) is mischarged *holo*EntB,^{1,6,17} which in principle can be formed by the phosphopantetheinyl transferase (EntD)-catalyzed reaction of an acyl-CoA or aroyl-CoA (in place of CoA) with EntB, or by the ATP-dependent *holo*EntB-catalyzed aroylation

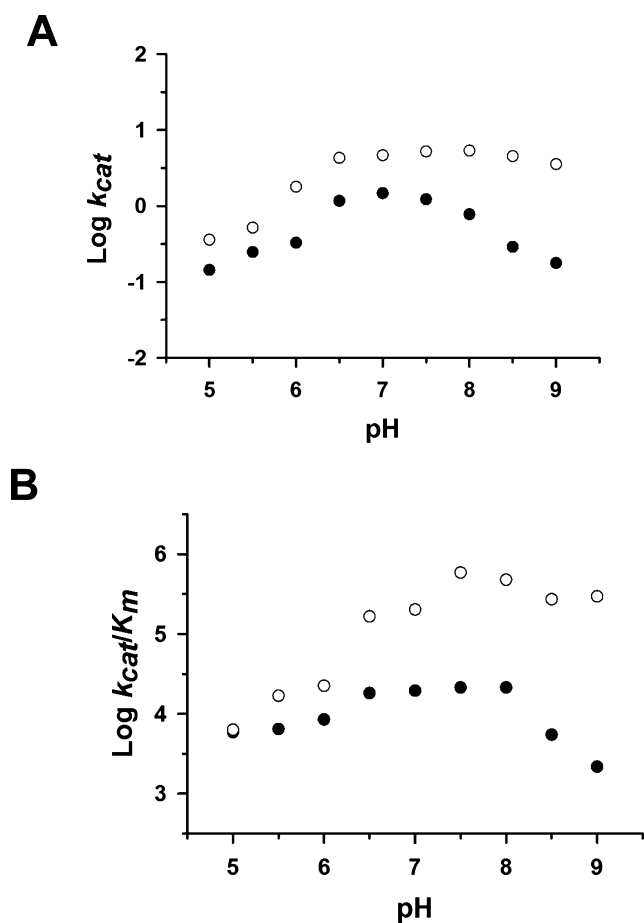
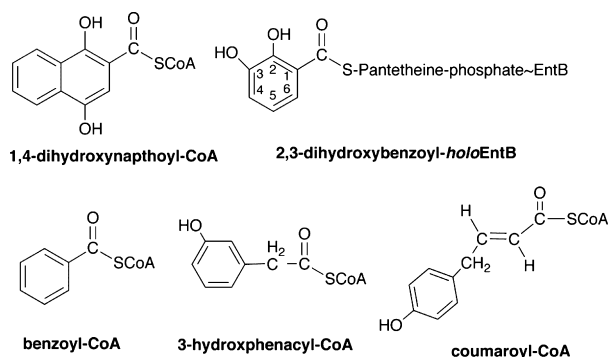


Figure 1. Plots of (A) $\log k_{cat}$ or (B) $\log k_{cat}/K_m$ measured for YdiI (○) and YdbB (●) catalyzed hydrolysis of 4-hydroxybenzoyl-CoA at 25 °C.

Chart 1. Structures of Representative Thioesters Tested in the YdbB and YdiI Substrate Activity Screen



with an aberrant (hydroxy)benzoate^c in place of the native substrate 2,3-dihydroxybenzoate¹ (Figure 2B). In our previous study,¹⁷ YdbB was shown to be highly active toward the enterobactin pathway intermediate 2,3-dihydroxybenzoyl-*holoEntB* ($k_{cat} = 2.8 \text{ s}^{-1}$, $k_{cat}/K_m = 1.8 \times 10^5 \text{ M}^{-1} \text{ s}^{-1}$) and toward the ring hydroxyl positional isomer 2,4-dihydroxybenzoyl-*holoEntB* ($k_{cat} = 3.7 \text{ s}^{-1}$, $k_{cat}/K_m = 1.4 \times 10^5 \text{ M}^{-1} \text{ s}^{-1}$), whereas the activity observed toward lauryl-*holoEntB* was found to be significantly lower ($k_{cat} = 0.1 \text{ s}^{-1}$, $k_{cat}/K_m = 6.3 \times 10^2 \text{ M}^{-1} \text{ s}^{-1}$). Thus, the proofreading function of YdbB appears to be primarily directed at stalled aroyl-*holoEntB* adducts. We also showed that benzoyl, 3-hydroxybenzoyl, and 4-hydroxybenzoyl-

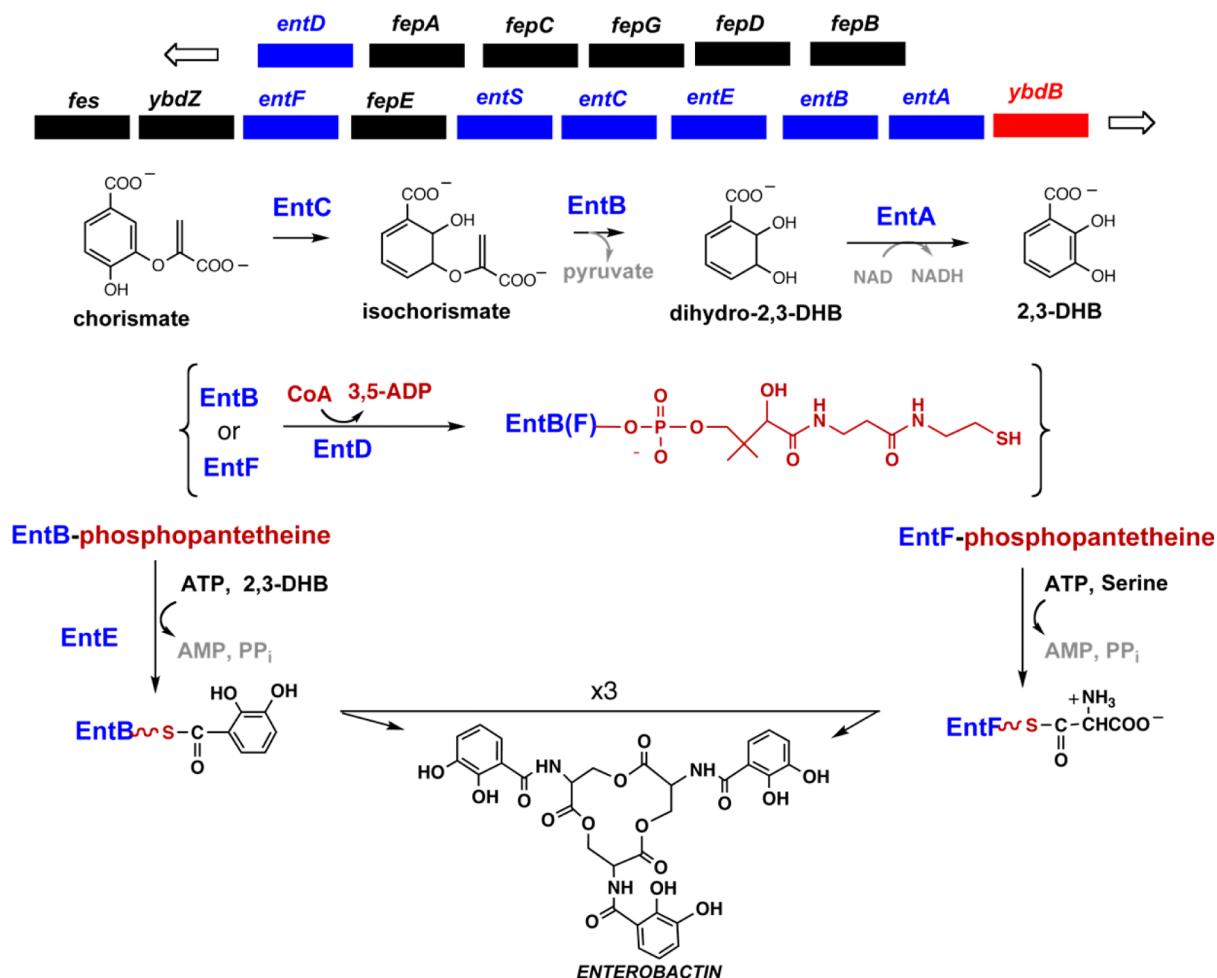
CoA are highly active YdbB substrates (k_{cat} values are 2.2, 1.2, and 1.6 s^{-1} , and k_{cat}/K_m values are 1.8×10^5 , 3.4×10^4 , and $7.6 \times 10^4 \text{ M}^{-1} \text{ s}^{-1}$)¹⁷ as are 3-hydroxyphenylacetyl-CoA and coumaroyl-CoA (k_{cat} values are 2.1 and 0.82 s^{-1} , and k_{cat}/K_m values are 5.7×10^4 and $8.4 \times 10^4 \text{ M}^{-1} \text{ s}^{-1}$) (Table 1). In contrast, the small acyl-CoA thioesters tested (acetyl-, propionyl-, β -methylcrotonyl-, and β -methylmalonyl-CoA) showed minimal or no detectable substrate activity with YdbB, and the short-to-medium chain length (C6–C12) fatty acyl-CoA thioesters displayed low turnover rates (k_{cat} range 0.03 – 0.1 s^{-1}) and low k_{cat}/K_m values ($(5$ – $6) \times 10^2 \text{ M}^{-1} \text{ s}^{-1}$) (Table 1). The longer chain (C14–C18) fatty acyl-CoA thioesters also displayed low turnover rates (0.03 – 0.09 s^{-1}) but had modestly improved k_{cat}/K_m values ($(2$ – $7) \times 10^3 \text{ M}^{-1} \text{ s}^{-1}$) (Table 1). Together the results indicate that YdbB recognizes CoA, as well as *holoEntB*, as the thioester thiol moiety, and that aroyl- and phenyl-substituted acyl moieties are targeted whereas purely aliphatic acyl moieties are not. Hydroxylation of the substrate benzoyl ring does not appear to have a significant impact on activity.^c

Given that YdbB is compatible with both CoA and *holoEntB* as the substrate thioester moiety, we were curious to learn whether YdbB can distinguish between different cellular ACPs. Thus, the benzoyl adduct of the *holoACP* which functions in *E. coli* fatty acid synthesis was prepared for testing. In contrast to the cases of benzoyl-CoA and (hydroxy)benzoyl-*holoEntB*, benzoyl-*holoACP* ($k_{cat} = 0.013 \text{ s}^{-1}$, $k_{cat}/K_m = 2.2 \times 10^2 \text{ M}^{-1} \text{ s}^{-1}$) proved to be a very poor substrate (Table 1), thereby indicating that the YdbB substrate binding site is selective for the ACP domain of EntB.

As will be detailed in the section that follows, the physiological substrate of *E. coli* YdiI is the menquinone pathway intermediate 1,4-dihydroxynaphthoyl-CoA^{18,20} (Figure 3). We were therefore particularly interested in comparing the catalytic efficiency of YdbB and YdiI with this substrate. Whereas the YdiI activity with 1,4-dihydroxynaphthoyl-CoA proved to be high ($k_{cat} = 1.6 \text{ s}^{-1}$, $k_{cat}/K_m = 2.0 \times 10^5 \text{ M}^{-1} \text{ s}^{-1}$), the YdbB activity was quite low ($k_{cat} = 0.009 \text{ s}^{-1}$, $k_{cat}/K_m = 5.5 \times 10^2 \text{ M}^{-1} \text{ s}^{-1}$). Conversely, YdiI proved to be an ineffective catalyst for the hydrolysis of the *holoEntB* adducts 2,4-dihydroxybenzoyl-*holoEntB*, 2,3-dihydroxybenzoyl-*holoEntB*, and lauryl-*holoEntB*. Only 2,4-dihydroxybenzoyl-*holoEntB* was hydrolyzed, and this took place at a very slow rate ($k_{cat} = 0.0036 \text{ s}^{-1}$, $k_{cat}/K_m = 1.8 \times 10^1 \text{ M}^{-1} \text{ s}^{-1}$). YdiI catalyzed the hydrolysis of the benzoyl-*holoACP* (FAS) ($k_{cat} = 0.083 \text{ s}^{-1}$, $k_{cat}/K_m = 1.5 \times 10^3 \text{ M}^{-1} \text{ s}^{-1}$), yet at an efficiency that is two orders of magnitude lower than that observed with the corresponding CoA thioester, benzoyl-CoA ($k_{cat} = 17.7 \text{ s}^{-1}$, $k_{cat}/K_m = 7.1 \times 10^5 \text{ M}^{-1} \text{ s}^{-1}$).

Next, we tested the level of promiscuity that YdiI exhibits toward aroyl-CoA and acyl-CoA thioesters. Although YdiI was not active toward acetyl-CoA, a modest level of activity was observed with propionyl-CoA ($k_{cat} = 0.21 \text{ s}^{-1}$ and $k_{cat}/K_m = 1.7 \times 10^3 \text{ M}^{-1} \text{ s}^{-1}$) and the small, polar acyl-CoA thioesters tested, namely, β -methylcrotonyl-CoA and β -methylmalonyl-CoA ($k_{cat} = 0.50 \text{ s}^{-1}$ and 0.67 s^{-1} ; $k_{cat}/K_m = 7.3 \times 10^3 \text{ M}^{-1} \text{ s}^{-1}$ and $5.8 \times 10^3 \text{ M}^{-1} \text{ s}^{-1}$, respectively) (Table 1). The YdiI k_{cat}/K_m values measured for the short-to-long chain fatty acyl-CoA thioesters (C6–C18) (0.14 – $4.1 \times 10^5 \text{ M}^{-1} \text{ s}^{-1}$), on the other hand, were observed to be in the same range as the k_{cat}/K_m values measured for coumaroyl-CoA ($2.8 \times 10^5 \text{ M}^{-1} \text{ s}^{-1}$), benzoyl-CoA ($7.1 \times 10^5 \text{ M}^{-1} \text{ s}^{-1}$), and 4-hydroxybenzoyl-CoA ($5.8 \times 10^5 \text{ M}^{-1} \text{ s}^{-1}$). However, the YdiI k_{cat} values determined for the

A



B

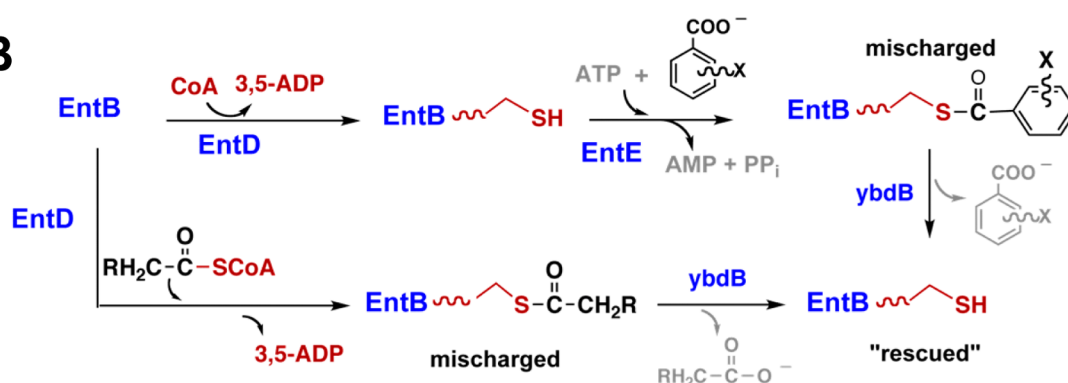


Figure 2. Summary of the *E. coli* enterobactin biosynthetic pathway. (A) Ordering of the clustered genes encoding the steps of the biosynthetic pathway (blue) and the genes encoding proteins involved in enterobactin transport and function (black). The proofreading hotdog-fold thioesterase YbdB gene is colored red. The chemical steps of the biosynthetic pathway catalyzed by the enzymes isochorismate synthase (EntC), bifunctional isochorismate lyase/aryl carrier protein (EntB), 2,3-dihydro-2,3-dihydroxybenzoate dehydrogenase (EntA), phosphopantetheinyltransferase component of entobacterin synthase multienzyme complex (EntD), enterobactin synthase component F (EntF), and 2,3 dihydroxybenzoate-AMP ligase (EntE). (B) Depiction of the mischarging of EntB catalyzed by EntD or *holoEntB* catalyzed EntE, and the EntB-regenerating thioester hydrolysis reaction (rescue) catalyzed by YbdB (aka EntH). In the figure, “R” can represent any organic group.

fatty acyl-CoA thioesters (range of $0.12\text{--}0.74\text{ s}^{-1}$) are significantly lower than the k_{cat} values measured for the phenyl ring-containing substrates (range of $5.2\text{--}17.7\text{ s}^{-1}$). A similar trend is observed with the YbdB k_{cat} values (Table 1). This finding suggests that productive binding is more likely to occur with an aroyl-thioester substrate than an acyl-thioester

substrate. The structural basis for this discrimination is provided in the companion paper.²

In summary, the comparison of the YbdB and YdiI substrate specificity profiles reveals that both thioesterases are (i) promiscuous, (ii) most active with benzoyl- and phenylacetyl-based thioester substrates, and (iii) significantly more active

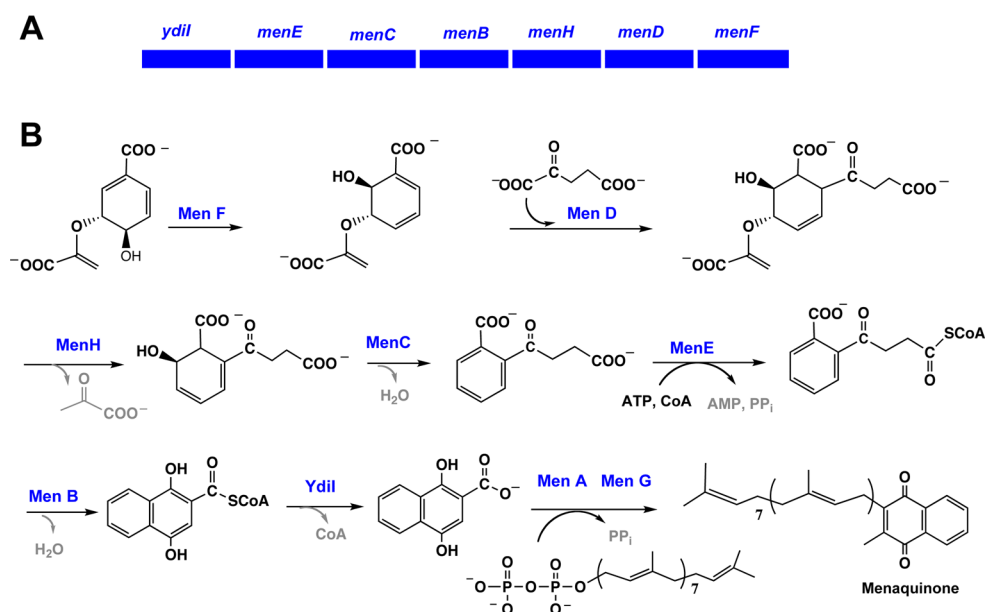


Figure 3. Menaquinone biosynthetic pathway. (A) The ordering of the clustered genes in the genome of *Tereadinibacter turnerae* T7901 is shown to illustrate the colocation of the *ydiI* with the pathway genes which is found in some bacterial species but does not occur in *E. coli*. (B) Reaction steps of the *E. coli* pathway catalyzed by upper pathway enzymes isochorismate synthase (MenF), 2-succinyl-5-enolpyruvyl-6-hydroxy-3-cyclohexene-1-carboxylate synthase (MenD), 2-succinyl-6-hydroxy-2,4-cyclohexadiene-1-carboxylate synthase (MenH), *o*-succinylbenzoate synthase (MenC), *o*-succinylbenzoic acid:CoA ligase (MenE), naphthoate synthase (MenB), 1,4-dihydroxy-2-naphthoyl-CoA thioesterase (YdiI), and lower pathway enzymes 1,4-dihydroxy-2-naphthoate octaprenyltransferase (MenA) and ubiquinone/menaquinone biosynthesis methyltransferase (MenG).

with a CoA-based thioester substrate than with the corresponding FAS *holo*ACP-based substrate. On the other hand, YbdB is highly active with EntB-based thioester substrates ($k_{\text{cat}}/K_m \sim 1 \times 10^5 \text{ M}^{-1} \text{ s}^{-1}$), whereas YdiI is not ($k_{\text{cat}}/K_m < 20 \text{ M}^{-1} \text{ s}^{-1}$), and conversely, YdiI is highly active with 1,4-dihydroxynaphthoyl-CoA ($k_{\text{cat}}/K_m = 2.0 \times 10^5 \text{ M}^{-1} \text{ s}^{-1}$) and fatty acyl-CoA thioester substrates ($k_{\text{cat}}/K_m \sim 1 \times 10^5 \text{ M}^{-1} \text{ s}^{-1}$), whereas YbdB is not ($k_{\text{cat}}/K_m = 5.5 \times 10^2 \text{ M}^{-1} \text{ s}^{-1}$ and $k_{\text{cat}}/K_m \sim 1 \times 10^3 \text{ M}^{-1} \text{ s}^{-1}$, respectively).

YdiI Biological Function. The findings from the gene neighborhood analysis reported in the section which follows revealed that only in some taxonomic groups of bacteria the YdiI/YbdB homolog gene is collocated with all (see, e.g., Figure 2A which depicts the *ydiI* gene neighborhood within the genome of *Tereadinibacter turnerae* T7901) or a partial set (e.g., species of *Bacteroides*¹⁹) of the genes encoding the menaquinone pathway enzymes. In *E. coli*, for example, *ydiI* is not collocated with the genes that support menaquinone synthesis. To demonstrate that YdiI is an essential catalyst for menaquinone synthesis in *E. coli*, the *ydiI* gene knockout mutant was subjected to two lines of investigation. First, Guo et al. showed that naphthoquinone production in this mutant was significantly reduced as compared to the parent strain.¹⁸ Second, in the present work, we measured the growth curves for wild-type *E. coli* cells and for the *ydiI* gene knockout mutant cells under conditions requiring anaerobic respiration. By serving as an electron transporter, menaquinone supports anaerobic respiration in facultative anaerobes such as *E. coli*. Precedent for our experiment is provided by previous work wherein it was shown that the disruption of menaquinone synthesis in *E. coli* via mutation of pathway gene *menB* or *menD* had no apparent impact on cell growth under aerobic conditions, whereas these mutant strains did not grow on glucose in the presence of fumarate, the ultimate electron acceptor, under anaerobic conditions.³⁰ As shown in Figure 4, the growth curves

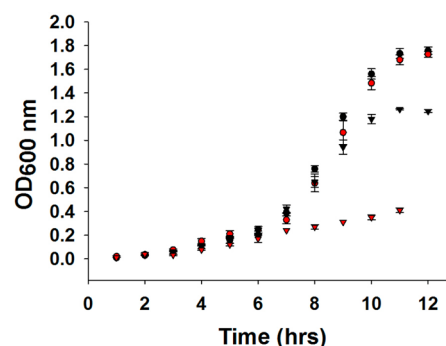


Figure 4. Comparison of the growth curves measured for *E. coli* wild-type (black circle) and the *E. coli* gene knockout mutant $\Delta ydiI$ (red circle) on glucose as the carbon source under aerobic conditions and for *E. coli* wild-type (black down triangle) and the *E. coli* gene-knockout mutant $\Delta ydiI$ (red down triangle) on glucose in the presence of fumarate under anaerobic conditions.

measured for wild-type *E. coli* K12 and the *ydiI*-knockout mutant grown on glucose under aerobic conditions are essentially identical. On the other hand, the comparison of the growth curves measured for wild-type *E. coli* K12 and the *ydiI*-knockout mutant grown anaerobically in the presence fumarate indicates that growth of the mutant cells is significantly inhibited (Figure 4). Thus, as in the case of the menaquinone pathway genes *menB* and *menD*, *ydiI* is required for growth under oxygen-limited conditions. Indeed, the NCBI GEO Profiles for YdiI reflect a significant increase observed in the expression of *ydiI* in *E. coli* cells grown under oxygen-limited conditions.³¹

Together with the high k_{cat}/K_m value of $2 \times 10^5 \text{ M}^{-1} \text{ s}^{-1}$ measured for YdiI-catalyzed conversion of 1,4-dihydroxynaphthoyl-CoA to 1,4-dihydroxynaphthoate, these findings provide

convincing evidence that YdiI mediates an essential step of the menaquinone biosynthetic pathway of *E. coli*.

Bioinformatic Analysis of the Divergence of the YdbB and YdiI. Ortholog Tracking. To identify homologs to *E. coli* YdiI and YdbB, BLAST searches of bacterial proteomes were carried out. In Table 2, we list the number of species per phyla

Table 2. Summary of the Number of Species That Encode a YdbB/YdiI Homolog and the Percent Sequence Identity (% SI) Shared with the *E. coli* YdiI Sequence^a

phylum/class	no. of species with homolog	range of % SI
Actinobacteria	29	41–53%
Bacteroidetes	82	36–64%
	28 fusion ^b	
Chlamydiae	1	51%
Chlorobi	11	45–49%
Chloroflexi	3	41–53%
Deinococci	12	40–52%
Firmicutes/Bacilli	70	37–55%
Firmicutes/Clostridia	7	45–50%
Proteobacteria/Alpha	3	47–50%
Proteobacteria/Beta	28	46–56%
Proteobacteria/Delta	5	35–56%
Proteobacteria/Gamma	297 + 40 ^c	37–99%

^aSee Table SI1 of Supporting Information for a listing of the individual species and protein accession codes. ^bThese homologs are fusion proteins which possess an N-terminal haloalkanoic acid dehalogenase (HAD) superfamily domain and a C-terminal YdiI-like domain.¹⁹ ^cThe number of species that possess a second YdbB/YdiI homolog.

and the percent sequence identity shared with the *E. coli* YdiI (see Table SI1 of the Supporting Information for an expanded list that gives statistics for each bacterial species). We discovered that the YdiI/YdbB homologs (as defined by sharing 35% or greater sequence identity) are spread throughout evolutionarily diverse bacterial phyla (viz., Acintobacteria, Bacteroidetes/Chlorobi, Chlamydiae, Firmicutes, and Proteobacteria) and that only the genomes of certain species of the genera of the family Enterobacteriaceae (order Enterobacteriales; class Gammaproteobacteria) encode two such homologs (see Table 3).

To assign biological function to the YdbB/YdiI homologs, we carried out additional BLAST searches using as queries the *E. coli* MenB, MenD, and MenE sequences to detect the menaquinone pathway, and the *E. coli* EntB, EntD, and EntF sequences to detect the enterobactin pathway.^d The occurrence of the enterobactin pathway enzymes was restricted to certain species of the Enterobacteriaceae family, each of which possesses two YdbB/YdiI homologs (see Table 3). On the other hand, the menaquinone pathway enzymes were found to be encoded by the genomes of most, yet not all, of the species that encode one or two YdbB/YdiI homologs (Table SI1 of the Supporting Information and Table 3).

Pursuant of our original goal to correlate divergence of YdbB/YdiI homolog function with the divergence of structure, we now take an in-depth look at the homologs within the Enterobacteriaceae family. In Table 3, we list the sequence identities of each YdbB/YdiI homolog with the *E. coli* YdiI and YdbB. Homologs, which share greater identity with the *E. coli* YdiI, than with the *E. coli* YdbB, are viewed as closer in lineage to the former than to the latter. In Table 3, we also list the “score cards” for the presence versus absence of the diagnostic

enzymes of the menaquinone and enterobactin pathways. In all but a few species (described below), we found that either all three enzymes of the pathway are present or none are, and based on this information we inferred the biological function of the homolog. With only a few exceptions, which are addressed below, the predicted lineage and biological function support the assignment of each homolog as ortholog to *E. coli* YdiI versus YdbB.

Specifically, the single YdbB/YdiI homolog found in species of the genera *Edwardsiella*, *Enterobacteriaceae* (sp. B9254FAA only), *Morganella*, *Proteus*, *Providencia*, *Rahnella*, *Phototribus*, and *Yersinia* (*pestis* KIM10+, *intermedia*, and *enterocolitica* only) has the highest sequence identity with the *E. coli* YdiI, and it is accompanied by the menaquinone pathway enzymes and not the enterobactin pathway enzymes. These particular homologs are assigned as *E. coli* YdiI orthologs (indicated in Table 3 by use of the bold font). Two YdbB/YdiI homologs are found in species of the genera *Citrobacter*, *Cronobacter*, *Escherichia*, *Salmonella*, *Raoultella*, *Shigella*, *Shimwellia*, *Enterobacteriaceae*, *Enterobacter*, and *Klebsiella* as are the respective sets of three diagnostic enzymes of the menaquinone and enterobactin pathways. In each case, the YdiI ortholog and YdbB ortholog can be clearly distinguished on the basis of the relative sequence identities with the *E. coli* paralogs.

Exceptions to the two scenarios presented above are attributed to the absence of one or more of the diagnostic menaquinone or enterobactin pathway enzymes. The genome of *Pantoea ananatis* LMG 5342, for instance, encodes a single YdbB/YdiI homolog, which shares equal (viz., 62%) sequence identity with the *E. coli* YdiI and YdbB, yet the genome does not encode the enzymes of the menaquinone or enterobactin pathway. The lineage and biological function are thus undefined. The genome of *Serratia symbiotica*, on the other hand, encodes pathway enzymes EntB, MenD, and MenB only, and a single YdbB/YdiI homolog, which shares 67% sequence identity with *E. coli* YdiI versus 54% with *E. coli* YdbB. In contrast, the other species *Serratia* listed in Table 3 possess all three (diagnostic) menaquinone pathway enzymes, yet only homologs to the enterobactin pathway enzymes EntB and EntF. The single YdbB/YdiI homolog produced in these species shares greater sequence identity with the *E. coli* YdiI (72–74%) than with the YdbB (54%). These data support the ortholog assignment YdiI for *Serratia* species *marcescens*, *odorifera*, *plymuthica*, *proteamaculans*, sp. AS12, and sp. D9; however, the function of the homolog from *Serratia symbiotica* remains undefined. The conservation of the EntB and EntF homologs among these species raises the possibility of the existence of an alternate siderophore biosynthetic pathway, which does not employ a YdbB-like housekeeper (i.e., EntB proofreader). An analogous scenario exists for two species *Xenorhabdus bovienii*, which possesses homologs to MenD, MenB, and MenE (hence, the menaquinone pathway) as well as to EntB and EntF (suggestive of a possible pathway leading to an alternate siderophore), and *Xenorhabdus nematophila*, which conserves the three diagnostic menaquinone pathway enzymes, but lacks the EntB and EntF homologs. As with *Xenorhabdus bovienii*, *Brenneria* sp. EniD312 possesses a single YdiI/YdbB homolog, which is most closely related in sequence to that of the *E. coli* YdiI (vs YdbB), and the three diagnostic menaquinone pathway enzymes plus the homologs to the *E. coli* EntB and EntF. Whereas we do not know the identity of the pathways that the EntB and EntF homologs of *Serratia*, *Xenorhabdus*, and *Brenneria* serve, the biosynthetic pathway

Table 3. Findings from the BLAST searches of the 173 Enterobacteriales Genomes Deposited in the NCBI Database Using the *E. coli* YbdB and YdiI Protein Sequences as Queries^a

genus ^{b,c}	species	no.	thioesterase(s)	Ent genes	Men genes	residue 68
<i>Brenneria</i>	sp. EniD312	1	YdiI (68) [YbdB (60)]	BFX	DBE	Val
<i>Citrobacter</i>	<i>koseri</i>	2	YbdB (93) and YdiI (91)	BFD	DBE	Met and Val
<i>Citrobacter</i>	<i>rodentium</i>	2	YbdB (94) and YdiI (89)	BFD	DBE	Met and Val
<i>Citrobacter</i>	sp. 30_2	2	YbdB (92) and YdiI (90)	BFD	DBE	Met and Val
<i>Citrobacter</i>	<i>youngae</i>	2	YbdB (94) and YdiI (86)	BFD	DBE	Met and Val
<i>Cronobacter</i>	<i>turcensis</i>	2	YbdB (81) and YdiI (76)	BFD	DBE	Met and Val
<i>Cronobacter</i>	<i>sakazaki</i>	2	YbdB (82) and YdiI (76)	BFD	DBE	Met and Val
<i>Dickeya</i>	<i>dadantii</i>	2	YbdB (57) ^c and YdiI (64)	BFX	DBE	Ile and Val
<i>Dickeya</i>	<i>zeae</i>	2	YbdB (57) ^c and YdiI (64)	BFX	DBE	Ile and Val
<i>Edwardsiella</i>	<i>ictturali</i>	1	YdiI (71) [YbdB (60)]	XXX	DBE	Leu
<i>Edwardsiella</i>	<i>tarda</i>	1	YdiI (71) [YbdB (60)]	XXX	DBE	Leu
<i>Enterobacter</i>	<i>asburiae</i>	2	YbdB (88) and YdiI (81)	BFD	DBE	Met and Val
<i>Enterobacter</i>	sp. R4-368, 638	2	YbdB (91) and YdiI (82)	BFD	DBE	Met and Val
<i>Enterobacter</i>	<i>cloacae</i>	2	YbdB (88) and YdiI (81)	BFD	DBE	Met and Val
<i>Enterobacter</i>	<i>hormaechei</i>	2	YbdB (89) and YdiI (80)	BFD	DBE	Met and Val
<i>Enterobacter</i>	<i>lignolyticus</i>	2	YbdB (89) and YdiI (78)	BFD	DBE	Met and Val
<i>Enterobacter</i>	<i>cancerogenus</i>	2	YbdB (89) and YdiI (79)	BFD	DBE	Met and Val
<i>Enterobacter</i>	<i>aerogenes</i>	2	YbdB (85) and YdiI (79)	BFD	DBE	Met and Val
<i>Enterobacteriaceae</i>	bacterium FGI 57	2	YbdB (92) and YdiI (76)	BFD	DBE	Met and Met
<i>Enterobacteriaceae</i>	bacterium 92S4FAA	1	YdiI (76) [YbdB (60)]	XXX	DBE	Leu
<i>Erwinia</i>	<i>billingsiae</i> Eb661	1	YdiI (67) [YbdB (60)]	XXX	DBE	Met
<i>Escherichia</i>	<i>albertii</i>	2	YbdB (99) and YdiI (93)	BFD	DBE	Met and Ile
<i>Escherichia</i>	<i>coli</i>	2	YbdB (100) and YdiI (100)	BFD	DBE	Met and Val
<i>Escherichia</i>	<i>fergusonii</i>	2	YbdB (100) and YdiI (86)	BFD	DBE	Met and Val
<i>Klebsiella</i>	<i>oxytoca</i>	2	YbdB (86) and YdiI (82)	BFD	DBE	Met and Val
<i>Klebsiella</i>	<i>pneumoniae</i>	2	YbdB (92) and YdiI (82)	BFD	DBE	Met and Val
<i>Morganella</i>	<i>morganii</i>	1	YdiI (68) [YbdB (60)]	XXX	DBE	Val
<i>Pantoea</i>	<i>ananatis</i> LMG 5342	1	YbdB (62) nor YdiI (62)	XXX	XXX	Val
<i>Pantoea</i>	<i>vagans</i> C91	1	YbdB (59) nor YdiI (63)	BFX	XXX	Ile
<i>Pantoea</i>	sp. At-9B	1	YbdB (61) nor YdiI (63)	BFX	XXX	Ile
<i>Pectobacterium</i>	<i>carotovorum</i>	1	YdiI (70) [YbdB (59)]	BfX ^d	DBE	Val
<i>Pectobacterium</i>	<i>wasabiae</i>	1	YdiI (69) [YbdB (59)]	BfX ^d	DBE	Val
<i>Pectobacterium</i>	<i>atrosepticum</i>	1	YdiI (69) [YbdB (59)]	BfX ^d	DBE	Val
<i>Pectobacterium</i>	sp. SCC3193	1	YdiI (69) [YbdB (59)]	BfX ^d	DBE	Val
<i>Photobacterium</i>	<i>asymbiotica</i>	1	YdiI (70) [YbdB (56)]	BXX	DBE	Leu
<i>Photobacterium</i>	<i>luminescens</i>	1	YdiI (70) [YbdB (57)]	BXX	DBE	Leu
<i>Proteus</i>	<i>mirabilis</i>	1	YdiI (71) [YbdB (1)]	XXX	DBE	Ile
<i>Proteus</i>	<i>penneri</i>	1	YdiI (72) [YbdB (59)]	XXX	DBE	Val
<i>Providencia</i>	<i>alcalifaciens</i>	1	YdiI (76) [YbdB (57)]	XXX	DBE	Leu
<i>Providencia</i>	<i>rettgeri</i>	1	YdiI (71) [YbdB (58)]	XXX	DBE	Ile
<i>Providencia</i>	<i>rustigianii</i>	1	YdiI (71) [YbdB (57)]	XXX	DBE	Ile
<i>Providencia</i>	<i>stuartii</i>	1	YdiI (71) [YbdB (57)]	XXX	DBE	Ile
<i>Rahnella</i>	<i>aquatilis</i>	1	YdiI (69) [YbdB (56)]	XXX	DBE	Met
<i>Rahnella</i>	sp. Y9602	1	YdiI (69) [YbdB (56)]	XXX	DBE	Met
<i>Raoultella</i>	<i>ornithinolytica</i>	2	YbdB (85) and YdiI (82)	BFD	DBE	Met and Val
<i>Samonella</i>	<i>enterica</i>	2	YbdB (92) and YdiI (90)	BFD	DBE	Met and Val
<i>Samonella</i>	<i>bongori</i>	2	YbdB (91) and YdiI (86)	BFD	DBE	Met and Val
<i>Serratia</i>	<i>marcescens</i>	1	YdiI (72) [YbdB (59)]	BFX	DBE	Met
<i>Serratia</i>	<i>odorifera</i>	1	YdiI (74) [YbdB (59)]	BFX	DBE	Met
<i>Serratia</i>	<i>plymuthica</i>	1	YdiI (73) [YbdB (59)]	BFX	DBE	Met
<i>Serratia</i>	<i>proteamaculans</i>	1	YdiI (74) [YbdB (59)]	BFX	DBE	Met
<i>Serratia</i>	<i>symbiotica</i>	1	YdiI (67) nor YbdB (54)	BXX	DBX	Ile
<i>Serratia</i>	sp. AS12	1	YdiI (73) [YbdB (59)]	BFX	DBE	Met
<i>Shigella</i>	sp. D9	2	YdiI (100) and YbdB (99)	BFX	DBE	Met and Val
<i>Shigella</i>	<i>flexneri</i>	2	YdiI (99) and YbdB (99)	BFD	DBE	Met and Val
<i>Shigella</i>	<i>dysenteriae</i>	2	YdiI (99) and YbdB (99)	BFD	DBE	Met and Val
<i>Shigella boydii</i>	boYdiI Sb227	2	YdiI (99) and YbdB (100)	BFD	DBE	Met and Val
<i>Shigella</i>	<i>sonnei</i> 53G	2	YdiI (99) and YbdB (99)	BFD	DBE	Met and Val
<i>Shimwellia</i>	<i>blattae</i>	2	YdiI (73) and YbdB (74)	BFX	DBE	Met and Val
<i>Xenorhabdus</i>	<i>bovienii</i>	1	YdiI (65) [YbdB (54)]	BFX	DBE	Leu

Table 3. continued

genus ^{b,c}	species	no.	thioesterase(s)	Ent genes	Men genes	residue 68
<i>Xenorhabdus</i>	<i>nematophila</i>	1	YdiI (72) [YbdB (59)]	XXX	DBE	Phe
<i>Yersinia</i>	<i>aldovae</i>	1	YdiI (68) nor YbdB (63)	XXX	DXE	Met
<i>Yersinia</i>	<i>bercovieri</i>	1	YdiI (68) nor YbdB (63)	XXX	DXE	Met
<i>Yersinia</i>	<i>enterocolitica</i>	1	YdiI (68) [YbdB (63)]	XXX	DBE	Met
<i>Yersinia</i>	<i>frederiksenii</i>	1	YdiI (65) nor YbdB (62)	BFX	DXE	Met
<i>Yersinia</i>	<i>intermedia</i>	1	YdiI (69) [YbdB (60)]	XXX	DBE	Met
<i>Yersinia</i>	<i>kristensenii</i>	1	YdiI (68) nor YbdB (62)	BFX	DXE	Met
<i>Yersinia</i>	<i>mollaretii</i>	1	YdiI (70) nor YbdB (61)	XXX	DXE	Met
<i>Yersinia</i>	<i>pestis</i> KIM10+	1	YdiI (70) [YbdB (62)]	XXX	DBE	Met

^aListed under the column heading “no.” is the number of YbdB and YdiI sequence homologs found having sequence identities >50% over >85% coverage. Reported under the column heading “thioesterases” are the sequence identities determined for the single homologs aligned separately with the *E. coli* YbdB and YdiI, and listed within the respective parentheses. In cases of two homologs, the reported sequence identity reflects that determined using the most homologous *E. coli* sequence. Ortholog assignment is indicated by bold font. The term “nor” is used to indicate that function not known, and ortholog assignment is not made. The column headings “Ent genes” and “Men genes” denote the presence of probable orthologs to the three diagnostic enterobactin pathway genes (*entB*, *entF*, and *entD*), represented as B, F, D, and to the three diagnostic menaquinone pathway genes (*menD*, *menB*, and *menE*), represented as D, B, E, respectively. An absent gene is represented using “X”. The probable orthologs were identified by BLAST searches of the individual proteomes using the respective *E. coli* pathway enzyme sequences as query, coupled with the criteria of >40% pairwise sequence identity for >85% coverage. See text for description of residue 68. See Table S12 of the Supporting Information for protein accession codes. ^bBacterial species found not to possess YbdB/YdiI homolog genes include *Buchnera aphidicola* str. Sg (*Schizaphis graminum*); *Blochmannia chromaiodes*, *pennsylvanicus*, and *vaferr*; *Hamiltonella defensa*; *Morganella endobia*; *Riesia pediculicola*; *Erwinia amylovora*, *chrysanthemi*, *pyrifoliae*, sp. Ejp617, and *tasmaniensis*; *Klebsilla variicola*, sp. 1 1 55, sp. 4 1 44FAA, sp. KTE92, sp. MS 92–3, and sp. OBRC7; *Sodalis glossinidius*; *Wigglesworthia glossinidia*; *Yersinia pseudotuberculosis*, *ruckeri*, *massiliensis*; *Yersinia pestis* biovar microtus str. 91001, *medievalis* str. harbin 35. ^cPosited to function as proofreader in in chrysobactin biosynthetic pathway ^dThe *E. coli* EntF shares ~40% identity with this homolog labeled “f”, which is a component of the biosynthetic pathway leading to the nonribosomal peptide pyoverdine.

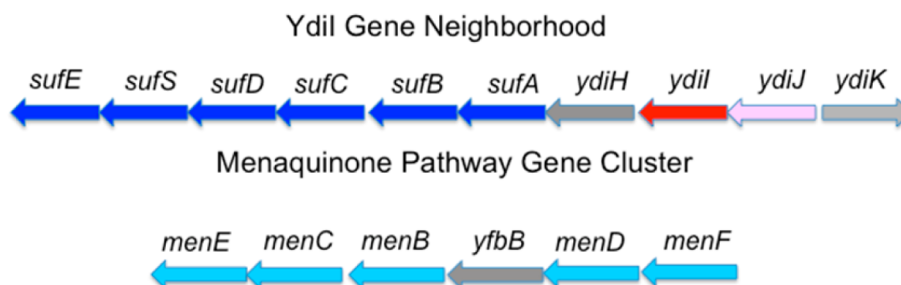


Figure 5. *E. coli* *ydiI* gene neighborhood (top) and the menaquinone pathway gene cluster (bottom). The arrows indicate the direction of gene transcription.

leading to the nonribosomal peptide pyoverdine is the likely home of the EntB and EntF homologs of *Pectobacterium*. The represented species of *Pectobacterium* possess the menaquinone pathway in which the single YdiI/YbdB homolog, which is most closely related in sequence to that of the *E. coli* YdiI (vs YbdB), is predicted to function. In summary, the YdiI/YbdB homologs of *Serratia*, *Xenorhabdus*, and *Brenneria* are assigned as YdiI orthologs.

Notably, the two representative species of the genus *Dickeya* synthesize chrysobactin³² in place of enterobactin. The two siderophores are structurally similar; both contain 2,3-dihydroxybenzoate and L-serine modules. Chrysobactin biosynthesis utilizes homologs to the enterobactin pathway synthases EntB and EntF, and we might expect that one of the two encoded YdiI/YbdB homologs has a proofreading role in chrysobactin biosynthesis similar to that performed by the *E. coli* YbdB in support of enterobactin biosynthesis. This YdiI/YbdB homolog is significantly more distant from the *E. coli* YbdB (57% sequence identity) than are the assigned YbdB orthologs (>80% sequence identity) (Table 3). The other YdiI/YbdB homolog of *Dickeya* shares 64% sequence identity with the *E. coli* YdiI and is predicted to function in the encoded

menaquinone pathway, consistent with its assignment as an ortholog to the *E. coli* YdiI.

The species of the genus *Yersinia* show the greatest variation with regard to their utilization of the YdiI/YbdB homolog. For instance, we did not find a homolog encoded by the genomes of *Yersinia pseudotuberculosis*, *ruckeri*, and *massiliensis*, or by the genomes of *Yersinia pestis* biovar microtus str. 91001 and *medievalis* str. harbin 35. On the other hand, the YdiI/YbdB homolog, which is most closely matched with the *E. coli* YdiI (68–70% sequence identity), coexists with the menaquinone pathway in *Yersinia pestis* KIM10+, *intermedia*, and *enterocolitica* and is thus assigned as a YdiI ortholog. The YdiI/YbdB homologs of *Yersinia aldovae*, *bercovieri*, and *mollaretii* are missing MenB, and all three enterobactin pathway enzymes. *Yersinia frederiksenii* and *kristensenii* are missing MenB and EntD. The higher sequence identity of these homologs with the *E. coli* YdiI (vs YbdB) suggests their lineage; however, their functions are not defined.

Gene Context. The genes encoding the proteins involved in the synthesis of 2,3-dihydroxybenzoate, the assembly of enterobactin, as well as its transport and cleavage are clustered on the *E. coli* genome along with *ybdB* (see Figure 2). The *ybdB* orthologs of other species of Enterobacteriaceae (Table 3) are

Table 4. Steady-State Kinetic Constants for Mutant YdiI- and YbdB-Catalyzed Hydrolysis of Benzoyl-CoA, Lauroyl-CoA, and 1,4-Dihydroxynaphthoyl-CoA Measured at pH 7.5 and 25 °C

	benzoyl-CoA			1,4-dihydroxynaphthoyl-CoA			lauroyl-CoA		
	k_{cat} (s ⁻¹)	K_m (μM)	k_{cat}/K_m (M ⁻¹ s ⁻¹)	k_{cat} (s ⁻¹)	K_m (μM)	k_{cat}/K_m (M ⁻¹ s ⁻¹)	k_{cat} (s ⁻¹)	K_m (μM)	k_{cat}/K_m (M ⁻¹ s ⁻¹)
YbdB									
WT ^a	2.2 ± 0.1	12 ± 1	1.8 × 10 ⁵	0.0093 ± 0.002	16 ± 2	5.8 × 10 ²	0.028 ± 0.002	44 ± 2	6.4 × 10 ²
M68V	1.8 ± 0.1	24 ± 2	7.5 × 10 ⁴	0.16 ± 0.02	5.9 ± 0.6	2.7 × 10 ⁴	0.046 ± 0.004	10.4 ± 0.3	4.5 × 10 ³
YdiI									
WT ^a	18 ± 1	25 ± 3	7.2 × 10 ⁵	1.6 ± 0.1	8 ± 1	2.0 × 10 ⁵	0.74 ± 0.01	2.2 ± 0.2	3.4 × 10 ⁵
V68M	28 ± 1	27 ± 2	1.0 × 10 ⁶	0.8 ± 0.1	2.0 ± 0.2	4.0 × 10 ⁵	0.77 ± 0.03	28 ± 2	2.8 × 10 ⁴
Y71A	28 ± 1	61 ± 4	4.6 × 10 ⁵	ND ^b	ND ^b	ND ^b	0.95 ± 0.02	3.4 ± 0.2	2.8 × 10 ⁵

^aWT stands for wild-type. ^bND stands for not determined.

also clustered with enterobactin pathway genes (see Figures SI1 and SI3 of the Supporting Information). Interestingly, the genes encoding the chrysobactin pathway proteins in *Dickeya dadantii* (and *zea*) are likewise clustered with the gene encoding the homolog to the YbdB of the enterobactin pathway (Figure SI3).

Oddly, the genes encoding the menaquinone pathway in *E. coli* are not colocated with *ydiI* (Figure 5). Instead, located downstream of the YdiI gene is a gene (*ydiJ* in *E. coli*) which encodes a large (1018 amino acids) multidomain protein annotated in EcoGene as a FAD-linked, 4Fe-4S cluster-containing oxidoreductase of unknown function. Located upstream is the *suf* operon, the protein products of which function in Fe-S cluster assembly under conditions of iron starvation or oxidative stress³³ (Figure 5). This gene context is largely conserved within Enterobacteriaceae;⁶ however, outside this taxonomic group, the gene context is highly varied, and numerous examples can be found where YdiI and the menaquinone pathway genes are colocated (see Figure 2 and Figures SI2 and SI4 of the Supporting Information).

YbdB and YdiI Sequence Markers. Based on the respective three-dimensional structures reported in the companion paper,² we identified amino acids 15, 68, and 71 as points of divergence in the respective *E. coli* YbdB and YdiI active site regions that accommodate the substrate aryl/alkyl group. For *E. coli* YbdB versus YdiI, the residues are Thr15 versus Met15, Met68 versus Val68, and Phe71 versus Tyr71, respectively. To determine if these residues are conserved, the amino acid sequences of the YbdB orthologs derived from Enterobacteriaceae species (Table 3) were aligned, as were the YdiI orthologs. The resulting multiple sequence alignments are shown in Figures SI5 and SI6 of the Supporting Information. The YbdB sequence alignment reveals high conservation of Met68 and Thr15 and conservative replacement of Phe71 (with Tyr or Trp). Two outliers are the YbdB homologs of the *Dickeya zeae* and *dadanti*, which are presumed to function in the chrysobactin biosynthetic pathway.³² These homologs share 60% pairwise sequence identity with the *E. coli* YbdB and possess Met15, Val68, and Trp71. A third outlier is the YbdB homolog of *Shimwellia blattae* (74% pairwise sequence identity with *E. coli* YbdB), as it possesses Met15, Met68, and Phe71. The residue at position 15 in YdiI is variable (the *E. coli* YdiI Met15 is replaced with polar residues as well as nonpolar residues), the *E. coli* YbdB Val68 is conservatively replaced with Met, Leu, or Ile, and the Tyr71 is stringently conserved. Notably, the strict conservation of YdiI Tyr71 is not required for efficient catalysis as revealed by the high (wild-type level) activity of the YdiI Y71A mutant (Table 4).

Despite some variation in the identity of the amino acid at position 68 in YdiI, based on structural considerations, we posit that this position is most closely linked to substrate binding. Specifically, the structures of the *E. coli* paralogs (see the companion paper²) show that Met68 in YbdB and Val68 in YdiI are located at the back of the alkyl/aryl binding pocket. To examine the importance of these residues to substrate recognition, the “residue-swapped” site-directed mutants YbdB M68V and YdiI V68M were prepared, and subjected to steady-state kinetic analysis (see Table 4 for the kinetic constants). The substrates tested with these mutants are benzoyl-CoA (highly active substrate for both YbdB and YdiI), 1,4-dihydroxynaphthoyl-CoA (highly active substrate for YdiI but not YbdB), and lauroyl-CoA (highly active substrate for YdiI but not YbdB). The k_{cat}/K_m values measured for YbdB M68V and YdiI V68M catalyzed-hydrolysis of benzoyl-CoA are essentially the same as those measured for the wild-type enzymes. In contrast, the k_{cat}/K_m value measured for YbdB M68V with 1,4-dihydroxynaphthoyl-CoA serving as substrate ($2.7 \times 10^4 \text{ M}^{-1} \text{ s}^{-1}$) is 47-fold larger than that measured with wild-type YbdB. The k_{cat}/K_m value measured for YdiI V68M with 1,4-dihydroxynaphthoyl-CoA serving as substrate is essentially unchanged. With lauroyl-CoA serving as substrate, the k_{cat}/K_m determined for YdiI V68M is reduced ~10-fold in value whereas the k_{cat}/K_m value measured for YbdB M68V ($4.5 \times 10^3 \text{ M}^{-1} \text{ s}^{-1}$) is increased ~10-fold. Thus, the comparatively lower catalytic efficiency of YbdB with the larger alkyl- and aryl-substituted substrates can be explained, at least in part, by the steric constraints imposed by the Met68.

CONCLUSION

We have shown that the biological range of YbdB is restricted to species of the family Enterobacteriaceae, whereas that of YdiI extends well beyond this, to other divisions of Proteobacteria as well as to other phyla (see Figure 6). The high overall sequence identity between *E. coli* YbdB and YdiI (59%) indicates that they are paralogs. Whereas YdiI is found in the vast majority of represented Enterobacteriaceae species, either alone or in combination with YbdB, the occurrence of YbdB is more restricted and coincides with that of YdiI. Indeed, whereas the siderophore enterobactin is unique to Enterobacteriaceae species, the electron acceptor menaquinone is required by a wide range of facultative anaerobes, including most species of Enterobacteriaceae. Thus, a reasonable scenario is that YbdB evolved within Enterobacteriaceae via divergence of an ancestral gene possibly following its duplication or horizontal transfer.^{34,35}

The YbdB and YdiI substrate specificity profiles (Table 1) show that both enzymes possess a high level of promiscuity,

The aroyl-binding site of YbdB does not accept the naphthoyl group, which we have shown for the *E. coli* enzyme can be attributed, at least in part, to Met68. Conversely, YdiI does not recognize EntB, and this suggests that there are important differences in the structures of the respective regions that accommodate the CoA nucleotide in both enzymes, and the EntB in YbdB only. To gain insight into the structural determinants, which support the divergence in YbdB and YdiI substrate specificity, the X-ray structure determinations reported in the companion paper² were carried out.

■ ASSOCIATED CONTENT

■ Supporting Information

Tables SI1 and SI2 and Figures SI1–SI6 showing the gene context and sequence alignment of Enterobacteriaceae YbdB orthologs and YdiI orthologs. This material is available free of charge via the Internet at <http://pubs.acs.org>.

■ AUTHOR INFORMATION

Corresponding Author

*Tel. 505-277-3383. Fax. 505-277-2609. E-mail: dd39@unm.edu.

Funding

This work was supported by NIH Grant GM 28688.

Notes

The authors declare no competing financial interest.

■ ABBREVIATIONS

CoA, coenzyme A; HB-CoA, hydroxybenzoyl-CoA; DHN-CoA, dihydroxynaphthoyl-CoA; HPA-CoA, hydroxyphenylacetyl-CoA; DHB-EntB, dihydroxybenzoyl-EntB; MES, 2-(*N*-morpholino)ethanesulfonate; HEPES, *N*-(2-hydroxyethyl)piperazine-*N'*-2-ethanesulfonate; TAPS, *N*-tris(hydroxymethyl)methyl-3-aminopropane sulfonate; CAPSO, 3-(cyclohexylamino)-2-hydroxy-1-propanesulfonate; DTNB, 5,5'-dithio-bis(2-nitrobenzoic acid)

■ ADDITIONAL NOTES

^aTerminology: Paralogous genes are created by a gene duplication event, whereas orthologous genes are genes in different species that originated by vertical descent from a single gene of the last common ancestor. Orthologous genes may or may not be functionally equivalent.

^bIn this paper, the term “*holo*” is used to specify that the ACP serine residue is functionalized with a phosphopantetheinyl group.

^cThis observation is different from that reported by Guo and co-workers.¹ We are not aware of the reason for the difference in substrate activity patterns.

^dThe enzymes were selected as the most diagnostic of the respective pathways because of the uniqueness of the reaction catalyzed (i.e., not common to other pathways) and/or their distinct structure (viz., no close sequence homologs having different functions).

^eThe significance, if any, of the YdiI gene context (viz., *ydiI*, *ydiH*, and the *suf* operon) conserved among the Enterobacteriaceae host species is unclear. However, it might be more than a coincidence that the gene neighborhood encodes a Fe-S cluster-dependent oxido-reductase, as well as Fe-S cluster assembly proteins, which are called into action when iron metabolism is disrupted.

^fWhereas the *E. coli* cells genetically engineered to overexpress *ybdB* showed inhibited growth upon iron starvation, the cells genetically engineered to overexpress YdiI did not.⁶ This suggests that YbdB will, at an abnormally high concentration, overtake EntF. Thus, strict regulation of the amount of YbdB present relative to the amount of EntF is to be expected.

■ REFERENCES

- (1) Guo, Z.-F., Sun, Y., Zheng, S., and Guo, Z. (2009) Preferential hydrolysis of aberrant intermediates by the type II thioesterase in *Escherichia coli* nonribosomal enterobactin synthesis: substrate specificities and mutagenic studies on the active-site residues. *Biochemistry* 48, 1712–1722.
- (2) Wu, R., Latham, J. A., Chen, D., Farelli, J. D., Zhao, H., Matthews, K., Allen, K. N., and Dunaway-Mariano, D. (2014) Structure and Catalysis in the *Escherichia coli* Hotdog-fold Thioesterase Paralog YdiI and YbdB. *Biochemistry*, DOI: 10.1021/bi500334v.
- (3) Zhuang, Z., Song, F., Takami, H., and Dunaway-Mariano, D. (2004) The BH1999 protein of *Bacillus halodurans* C-125 is gentisyl-coenzyme A thioesterase. *J. Bacteriol.* 186, 393–399.
- (4) Widhalm, J. R., van Oostende, C., Furt, F., and Basset, G. J. (2009) A dedicated thioesterase of the Hotdog-fold family is required for the biosynthesis of the naphthoquinone ring of vitamin K1. *Proc. Natl. Acad. Sci. U.S.A.* 106, 5599–5603.
- (5) Scholten, J. D., Chang, K. H., Babbitt, P. C., Charest, H., Sylvestre, M., and Dunaway-Mariano, D. (1991) Novel enzymic hydrolytic dehalogenation of a chlorinated aromatic. *Science* 253, 182–185.
- (6) Leduc, D., Battesti, A., and Bouveret, E. (2007) The hotdog thioesterase EntH (YbdB) plays a role in vivo in optimal enterobactin biosynthesis by interacting with the ArCP domain of EntB. *J. Bacteriol.* 189, 7112–7126.
- (7) Song, F., Zhuang, Z., Finci, L., Dunaway-Mariano, D., Kniewel, R., Buglino, J. A., Solorzano, V., Wu, J., and Lima, C. D. (2006) Structure, function, and mechanism of the phenylacetate pathway hot dog-fold thioesterase PaaI. *J. Biol. Chem.* 281, 11028–11038.
- (8) Weeks, A. M., and Chang, M. C. (2012) Catalytic control of enzymatic fluorine specificity. *Proc. Natl. Acad. Sci. U.S.A.* 109, 19667–19672.
- (9) Hunt, M. C., Siponen, M. I., and Alexson, S. E. (2012) The emerging role of acyl-CoA thioesterases and acyltransferases in regulating peroxisomal lipid metabolism. *Biochim. Biophys. Acta* 1822, 1397–1410.
- (10) Cohen, D. E. (2013) New Players on the Metabolic Stage: How Do You Like Them Acots? *Adipocyte* 2, 3–6.
- (11) Dillon, S. C., and Bateman, A. (2004) The Hotdog fold: wrapping up a superfamily of thioesterases and dehydratases. *BMC Bioinf.* 5, 109.
- (12) Ollis, D. L., Cheah, E., Cygler, M., Dijkstra, B., Frolow, F., Franken, S. M., Harel, M., Remington, S. J., Silman, I., Schragl, J., Sussman, J. L., and Goldmans, A. (1992) The α/β hydrolase fold. *Protein Eng.* 5, 197–211.
- (13) Benning, M. M., Wesenberg, G., Liu, R., Taylor, K. L., Dunaway-Mariano, D., and Holden, H. M. (1998) The three-dimensional structure of 4-hydroxybenzoyl-CoA thioesterase from *Pseudomonas* sp. Strain CBS-3. *J. Biol. Chem.* 273, 33572–33579.
- (14) Cao, J., Xu, H., Zhao, H., Gong, W., and Dunaway-Mariano, D. (2009) The mechanisms of human hotdog-fold thioesterase 2 (hTHEM2) substrate recognition and catalysis illuminated by a structure and function based analysis. *Biochemistry* 48, 1293–1304.
- (15) Smotrys, J. E., and Linder, M. E. (2004) Palmitoylation of intracellular signaling proteins: regulation and function. *Annu. Rev. Biochem.* 73, 559–587.
- (16) Khersonsky, O., and Tawfik, D. S. (2010) Enzyme promiscuity: a mechanistic and evolutionary perspective. *Annu. Rev. Biochem.* 79, 471–505.
- (17) Chen, D., Wu, R., Bryan, T. L., and Dunaway-Mariano, D. (2009) In vitro kinetic analysis of substrate specificity in enterobactin

biosynthetic lower pathway enzymes provides insight into the biochemical function of the hot dog-fold thioesterase EntH. *Biochemistry* 48, 511–513.

(18) Chen, M., Ma, X., Chen, X., Jiang, M., Song, H., and Guo, Z. (2013) Identification of a hotdog fold thioesterase involved in the biosynthesis of menaquinone in *Escherichia coli*. *J. Bacteriol.* 195, 2768–2775.

(19) Wang, M., Song, F., Wu, R., Allen, K. N., Mariano, P. S., and Dunaway-Mariano, D. (2013) Co-evolution of HAD phosphatase and hotdog-fold thioesterase domain function in the menaquinone-pathway fusion proteins BF1314 and PG1653. *FEBS Lett.* 587, 2851–2859.

(20) Latham, J. A. (2012) Structure to function: case studies of hotdog-fold superfamily thioesterases from *Escherichia coli*. PhD Thesis, University of New Mexico, pp 2–96.

(21) Luo, L., Taylor, K. L., Xiang, H., Wei, Y., Zhang, W., and Dunaway-Mariano, D. (2001) Role of active site binding interactions in 4-chlorobenzoyl-coenzyme A dehalogenase catalysis. *Biochemistry* 40, 15684–15692.

(22) Baba, T., Ara, T., Hasegawa, M., Takai, Y., Okumura, Y., Baba, M., Datsenko, K. a, Tomita, M., Wanner, B. L., and Mori, H. (2006) Construction of *Escherichia coli* K-12 in-frame, single-gene knockout mutants: the Keio collection. *Mol. Syst. Biol.*, DOI: 10.1038/msb4100049.

(23) Cronan, J. E., and Klages, A. L. (1981) Chemical synthesis of acyl thioesters of acyl carrier protein with native structure *Biochemistry. Proc. Natl. Acad. Sci. U.S.A.* 78, 5440–5444.

(24) Bradford, M. M. (1976) A rapid and sensitive method for the quantitation of microgram quantities of protein utilizing the principle of protein-dye binding. *Anal. Biochem.* 72, 248–254.

(25) Papadopoulos, J. S., and Agarwala, R. (2007) COBALT: constraint-based alignment tool for multiple protein sequences. *Bioinformatics* 23, 1073–1079.

(26) Gouet, P., Robert, X., and Courcelle, E. (2003) ESPript/ENDscript: extracting and rendering sequence and 3D information from atomic structures of proteins. *Nucleic Acids Res.* 31, 3320–3323.

(27) Taylor, K. L., Liu, R. Q., Liang, P. H., Price, J., Dunaway-Mariano, D., Tonge, P. J., Clarkson, J., and Carey, P. R. (1995) Evidence for electrophilic catalysis in the 4-chlorobenzoyl-CoA dehalogenase reaction: UV, Raman, and ¹³C-NMR spectral studies of dehalogenase complexes of benzoyl-CoA adducts. *Biochemistry* 34, 13881–13888.

(28) De Lay, N. R., and Cronan, J. E. (2007) *In vivo* functional analyses of the type II acyl carrier proteins of fatty acid biosynthesis. *J. Biol. Chem.* 282, 20319–20328.

(29) Gehring, A. M., Mori, I., and Walsh, C. T. (1998) Reconstitution and characterization of the *Escherichia coli* enterobactin synthetase from EntB, EntE, and EntF. *Biochemistry* 37, 2648–2659.

(30) Guest, J. R. (1979) Anaerobic growth of *Escherichia coli* K12 with fumarate as terminal electron acceptor: Genetic studies with menaquinone and fluoroacetate-resistant mutants. *J. Gen. Microbiol.* 115, 259–271.

(31) Sangurdekar, D. P., Srienc, F., and Khodursky, A. B. (2006) A classification based framework for quantitative description of large-scale microarray data. *Genome Biol.* 7, R32.

(32) Sandy, M., and Butler, A. (2011) Chrysobactin siderophores produced by *Dickeya chrysanthemi* EC16. *J. Nat. Prod.* 74, 1207–1212.

(33) Outten, F. W., Djaman, O., and Storz, G. (2004) A suf operon requirement for Fe-S cluster assembly during iron starvation in *Escherichia coli*. *Mol. Microbiol.* 52, 861–872.

(34) Taylor, J. S., and Raes, J. (2004) Duplication and divergence: The evolution of new genes and old ideas. *Annu. Rev. Genetics* 38, 615–643.

(35) Zhang, J. (2003) Evolution by gene duplication: An update. *Trends Ecol. Evol.* 18, 282–298.

(36) Brickman, T. J., Ozenberger, B. A., and McIntosh, M. A. (1990) Regulation of divergent transcription from the iron-responsive *fepB*-*entC* promoter-operator regions in *Escherichia coli*. *J. Mol. Biol.* 212, 669–682.